Spinor atom-molecule conversion via laser-induced three-body recombination

H. Jing,[1,2] Y. Deng,[1] and P. Meystre[2]
[1]*Department of Physics, Henan Normal University, Xinxiang 453007, China*
[2]*B2 Institute, Department of Physics and College of Optical Sciences, University of Arizona, Tucson, Arizona 85721, USA*
(Received 15 November 2010; revised manuscript received 22 January 2011; published 1 April 2011)

We study the theory of several aspects of the dynamics of coherent atom-molecule conversion in spin-one Bose-Einstein condensates. Specifically, we discuss how, for a suitable dark-state condition, the interplay of spin-exchange collisions and photo association leads to the stable creation of an atom-molecule pair from three initial spin-zero atoms. This process involves *two* two-body interactions and can be intuitively viewed as an effective three-body recombination. We investigate the relative roles of photo association and of the initial magnetization in the "resonant" case, where the dark-state condition is perfectly satisfied. We also consider the "nonresonant" case, where that condition is satisfied either only approximately—the so-called adiabatic case—or not at all. In the adiabatic case, we derive an effective nonrigid pendulum model that allows one to conveniently discuss the onset of an antiferromagnetic instability in an "atom-molecule pendulum," as well as large-amplitude pair oscillations and atom-molecule entanglement.

DOI: 10.1103/PhysRevA.83.043601 PACS number(s): 03.75.Pp, 42.50.−p, 03.70.+k

I. INTRODUCTION

Recent years have witnessed rapid advances in the manipulation of the spin degrees of freedom of ultracold atoms [1–6]. Through magnetic steering of two-body collisions, a broad range of effects have been observed, including atomic magnetism [7–10], coherent spin mixing [5,11], topological excitations [12], and an atomic analog of the Einstein–de Haas effect [13]. The *optical* control of atomic spin dynamics has also attracted much experimental interest [14–16]. For example, Dumke *et al.* [14] and Hamley *et al.* [15] investigated the photo-association (PA) diagnosis [14] and PA spectroscopy [15] of spin-one atoms, opening the way to studies of PA-controlled regular [17] or chaotic [18] spin dynamics.

In a very recent experiment, ro-vibrational ground-state molecules were successfully prepared via the all-optical association of laser-cooled atoms [19], which has triggered the investigation of coherent PA in a wide variety of ultracold atomic and molecular systems [20]. A result of particular relevance for the present study is an experiment by Kobayashi *et al.*, who used a coherent two-color PA technique to create spinor molecules in a spin-one atomic Bose condensate [16]. In particular, these authors found that for strong PA couplings, the atomic spin oscillations are significantly suppressed, and the dominant process is scalarlike atom-molecule conversion. That is, only the populations of the spin components that are associated into molecules are observed to decrease, while the other spin component remains almost unchanged on the experimentally relevant time scale [16].

In this paper, we show that under appropriate two-photon resonance conditions, quantum interference between optical PA and atomic spin mixing can lead to the existence of a dark state of the spin-down atoms, which can in turn be exploited for the stable formation of a spinor atom-molecule pair from three initial spin-zero atoms. This process, which involves *two* two-body interactions, can be thought of as an effective three-body spin-exchange effect. The important role of the initial magnetization in creating the atom-molecule pairs is also analyzed. We also analyze dynamical features that occur in the "nonresonant" regime, in which no dark state is formed; these dynamics include large-amplitude coherent oscillations of the atom-molecule pairs population and an antiferromagnetic instability. As such, these manifestations of the interplay between two-color PA and spin-exchange collisions allow insight into the study of quantum spin gases and ultracold chemistry [20].

The article is organized as follows. Section II discusses the resonant situation, where the dynamics of the system are characterized by the existence of a dark state. We first introduce our model, which we then apply to the description of scalarlike PA [16]. We then derive a dark-state condition for the spin-down atoms and show that, when satisfied, it results in the stable resonant creation of atom-molecule pairs. The role of the initial atomic magnetization is also discussed. Section III then turns to the nonresonant regime. We show that in that case, the system can be described in terms of a nonrigid pendulum model. Two important dynamical manifestations of this regime, large-amplitude atom-molecule oscillations and a regime of antiferromagnetic instability, are discussed. Finally, Sec. IV is a summary and conclusion.

II. THE MODEL

This section introduces our model and exploits it to describe the main features of scalarlike PA [16]. We also discuss a process of stable atom-molecule pair formation and analyze the role of the initial magnetization in the system dynamics.

A. Theoretical model

The system that we consider is illustrated in Fig. 1. It consists of a spin-one atomic condensate undergoing spin-changing two-body collisions and coupled via two-photon coherent PA to a ground-state diatomic molecular condensate.

If we denote by $\hat{\psi}_{i,j=0,\pm1}$ and $\hat{\psi}_{m,g}$ the annihilation operators of the three atomic components and of the excited- or ground-state molecules, respectively, the Hamiltonian of the binary atomic and molecular condensate (for $\hbar = 1$) is

$$\widehat{H} = \widehat{\mathcal{H}}_0 + \widehat{\mathcal{H}}_{\rm coll} + \widehat{\mathcal{H}}_{\rm PA}, \tag{1}$$

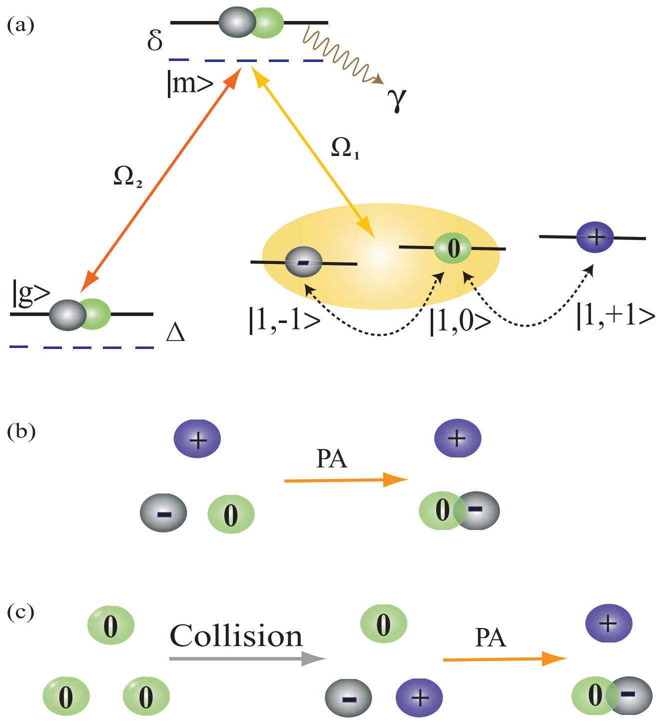

FIG. 1. (Color online) (a) Schematic of coherent two-color PA in a spin-one atomic condensate. Here, δ and Δ are the one- and two-photon detunings of the laser fields with Rabi frequencies $\Omega_{1,2}(t)$, and γ accounts for the spontaneous decay of the excited state $|m\rangle$. (b) Scalarlike atom-molecule conversion, as observed in a recent experiment by Kobayashi *et al.* [16]. (c) Effective three-body recombination resulting from the interplay of two interactions of two bodies (see text).

where

$$\widehat{\mathcal{H}}_0 = \int d\mathbf{r}\Bigg[\sum_{i=-1,0,1}\widehat{\psi}_i^\dagger(V+E_i)\widehat{\psi}_i + \left(\delta-\frac{1}{2}i\gamma\right)\widehat{\psi}_m^\dagger\widehat{\psi}_m + (\Delta+\delta)\widehat{\psi}_g^\dagger\widehat{\psi}_g\Bigg], \quad (2)$$

$$\widehat{\mathcal{H}}_{\rm coll} = \frac{1}{2}\int d\mathbf{r}\Big[c_0'\widehat{\psi}_i^\dagger\widehat{\psi}_j^\dagger\widehat{\psi}_j\widehat{\psi}_i + c_2'\widehat{\psi}_i^\dagger(F_\kappa)_{ij}\widehat{\psi}_j\widehat{\psi}_k^\dagger(F_\kappa)_{kl}\widehat{\psi}_l\Big], \quad (3)$$

$$\widehat{\mathcal{H}}_{\rm PA} = \int d\mathbf{r}[-\Omega_2\widehat{\psi}_g^\dagger\widehat{\psi}_m + \Omega_1\widehat{\psi}_m^\dagger\widehat{\psi}_0\widehat{\psi}_{-1} + \text{H.c.}]. \quad (4)$$

Here, V is the trap potential, E_i is the energy of the spin state i with a static magnetic field lifting its degeneracy, $F_{\kappa=x,y,z}$ are spin-one matrices, and

$$c_0' = 4\pi(a_0+2a_2)/3M$$

and

$$c_2' = 4\pi(a_2-a_0)/3M,$$

where $a_{0,2}$ are s-wave scattering lengths [8], Ω_i $(i=\{1,2\})$ are the Rabi frequencies of the PA fields, and γ is a phenomenological decay factor. The detunings δ and Δ between the PA fields and the atomic and molecular levels are defined in Fig. 1. We have ignored the kinetic energy of the particles by assuming a dilute ensemble. Note also that this model ignores molecular collisions, since there is currently no knowledge of their strength.

To extract the main aspects of the system dynamics, we invoke a single-mode approximation, a simplification that has proven successful in describing key aspects of related systems in the past [3,9,10]. It amounts to approximating the field operators of the three spin components of the atomic condensate as

$$\widehat{\psi}_i(\vec{r},t) = \sqrt{N}\hat{a}_i(t)\phi(\vec{r})\exp(-i\mu t/\hbar),$$

where N is the initial atomic number; μ is the chemical potential; $\phi(\vec{r})$ is the normalized condensate wave function for each spin component, satisfying $\int d\vec{r}|\phi(\vec{r})|^2 = 1$ [9,10]; and $\hat{a}_i(t)$ are bosonic annihilation operators. The molecular field is likewise described in a single-mode approximation, with the annihilation operators $\hat{m}$ and $\hat{g}$ describing excited and ground-sate molecules.

For large-enough detunings δ, the intermediate molecular state $|m\rangle$ can be adiabatically eliminated [21], simplifying the Heisenberg equations of motion of the atom-molecule system to

$$\begin{aligned} i\frac{d\hat{a}_+}{d\tau} &= \chi_2(\rho_+ + \rho_0 - \rho_-)\hat{a}_+ + \chi_2\hat{a}_0^2\hat{a}_-^\dagger,\\ i\frac{d\hat{a}_0}{d\tau} &= \chi_2(\rho_+ + \rho_-)\hat{a}_0 - \omega\rho_-\hat{a}_0 + 2\chi_2\hat{a}_+\hat{a}_-\hat{a}_0^\dagger + \Omega\hat{g}\hat{a}_-^\dagger,\\ i\frac{d\hat{a}_-}{d\tau} &= -\Gamma\hat{a}_- + \chi_2\hat{a}_0^2\hat{a}_+^\dagger + \Omega\hat{g}\hat{a}_0^\dagger,\\ i\frac{d\hat{g}}{d\tau} &= \Omega\hat{a}_0\hat{a}_- + (\Delta+\delta-\delta')\hat{g}. \end{aligned} \quad (5)$$

These equations will be treated in the following discussion by using the mean-field replacement $\hat{a}_i,\hat{g}\to\sqrt{\rho_{i,g}}$, with $\rho_i = |a_i|^2$ or $\rho_g = |g|^2$ denoting the atomic or molecular density [3]. The rescaled parameters in Eqs. (5) are

$$c_{0,2} = c_{0,2}'\int d\mathbf{r}|\phi(\mathbf{r})|^4, \quad (6)$$

$$\delta' = \frac{\Omega_2^2}{c_0N\delta}\left(1+\frac{i\gamma}{2\delta}\right), \quad (7)$$

and we have introduced the dimensionless variables $\tau = c_0Nt$, $\chi_2 = c_2/c_0$, $\omega = \Omega_1^2/(c_0N\delta)$, $\Gamma = \omega\rho_0 - \chi_2(\rho_- + \rho_0 - \rho_+)$, and $\Omega = \frac{\Omega_1\Omega_2}{c_0N\delta}$.

B. Scalarlike photo association

In their recent experiment on two-color PA of the spinor atoms ^{87}Rb [16], Kobayashi *et al.* observed the spin-selective formation of the molecular state $|2,-1\rangle$ from reactant atoms in the states $|1,-1\rangle$ and $|1,0\rangle$. One important feature of their experimental results is that while the populations of the reactant atoms decreased, the population of the state $|1,1\rangle$ remained almost unchanged. This is the situation illustrated in Fig. 1(b) [16].

To test our model against that experiment, we assume that the energy degeneracy of the atomic magnetic sublevels is lifted by a static magnetic field and that the atomic condensate

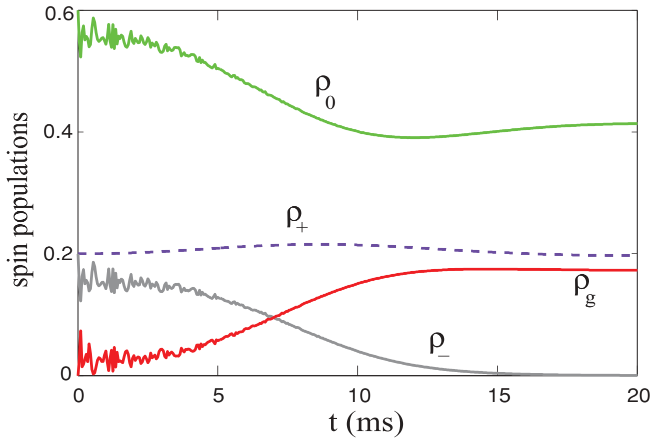

FIG. 2. (Color online) Scalarlike atom-molecule conversion of ^{87}Rb atoms, with an essentially unchanged population in the spin-up state [16]. The initial conditions are $f = [\sqrt{0.2},\sqrt{0.6},\sqrt{0.2}]$ and $\Omega = \Omega_m \mathrm{sech}(t/4)$, with $|\Omega_m/\chi_2| = 1.44 \times 10^4$ [16]. The other parameters are $\chi_2 = -0.01$, $\delta = -100\chi_2$, $\gamma = 10|\chi_2|$, and $c_0 N = 10^5\ \mathrm{s}^{-1}$.

is initially prepared in the state $f = [\sqrt{0.2},\sqrt{0.6},\sqrt{0.2}]$ [16]. The experiment used two lasers of maximum powers $I_1 = I_2/2 = 10$ W, detuning $\delta = 2\pi \times 300$ MHz, and $\Omega/\sqrt{I} = 7$ MHz $(\mathrm{W\,cm^{-2}})^{-\frac{1}{2}}$, which in our case yields $\Omega_1 = 139$ MHz and $\Omega_2 = 197$ MHz. As we will see in the following analysis, these values are well beyond the regime of atom-molecule pair formation, and as illustrated in Fig. 2, our model confirms that the two-color PA of atoms into molecules is scalarlike in this case.

C. Stable atom-molecule pair formation

The scalarlike PA sketched in the previous subsection results from the binding of a pair of Rb atoms of spin-zero and spin-down. We now consider the case of PA from spin zero, but in the presence of spin-changing collisions; this situation is sketched in Fig. 1(c). Specifically, we assume that the atomic condensate is initially prepared in the spin-zero state $|1,0\rangle$. Spin-exchange collisions then couple a pair of spin-zero atoms to a pair of atoms with opposite spins, $2A_0 \to A_\downarrow + A_\uparrow$ [15], while PA fields of appropriate wavelengths selectively combine a spin-down atom and a spin-zero atom into the molecular ground state $|g\rangle$ via a virtual transition to an excited molecular $|m\rangle$, $A_0 + A_\downarrow \to A_0A_\downarrow$ [16]. The outcome of these combined mechanisms is the creation of an atom-molecule pair from three spin-zero atoms, $3A_0 \to A_0A_\downarrow + A_\uparrow$, a process that can be intuitively thought of as an effective spin-dependent three-body recombination. As such, this process is quite different from both the scalarlike PA of the previous subsection [16] and purely atomic laser-catalyzed spin mixing [17].

In this case, we found numerically that stable atom-molecule pair formation is possible, provided that the dark-state condition

$$\Omega(t) = -\chi_2\sqrt{\frac{\rho_0\rho_+}{\rho_g}} \tag{8}$$

for the spin-down atomic state is satisfied [22,23]. This result is easily confirmed from Eqs. (5), which show that when condition (8) is satisfied, the spin-down atomic state remains essentially unoccupied. That situation is illustrated in Fig. 3, which shows the efficient stable creation of atom-molecule pairs in this case.

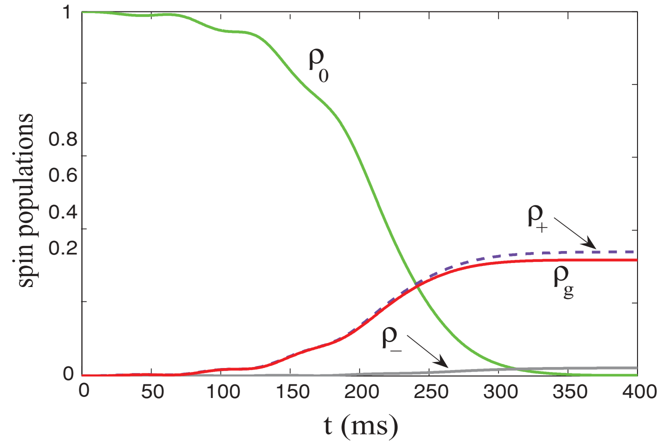

FIG. 3. (Color online) Atom-molecule pair formation as a function of time for ^{87}Rb atoms, under the dark-state condition for spin-down atoms. The initial state is $f = [0,1,0]$, and the other parameters are the same as in Fig. 2.

D. Role of magnetization

The initial magnetization

$$\mathcal{M} = \rho_+ - \rho_- - \rho_g \tag{9}$$

of a spin gas prepared in the state $f = [0,1,0]$ is $\mathcal{M} = 0$. In this subsection, we consider the role of that initial magnetization in the creation of atom-molecule pairs. We find that in contrast to the case of scalarlike molecule formation, the initial magnetization now plays a significant role, as illustrated in Figs. 4 and 5.

Figure 4 shows the evolution of the population of ground-state molecules for several values of the initial magnetization under the generalized dark-state condition (8). For $\mathcal{M} \geqslant 0$, the ground-state molecules are produced efficiently and reach a steady-state population $\rho_g = (1-\mathcal{M})/3$; for $\mathcal{M} < 0$, in

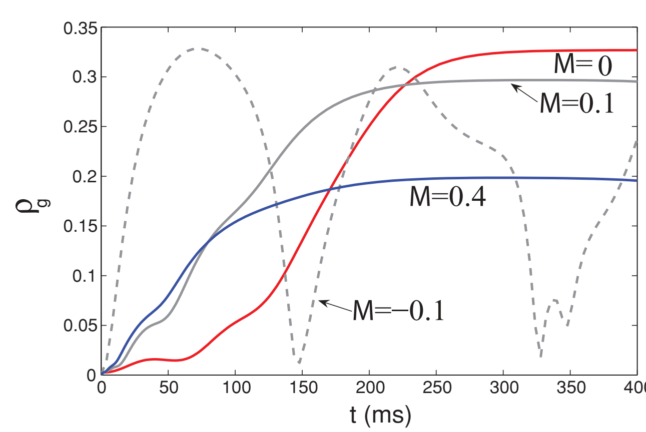

FIG. 4. (Color online) Spinor molecule population for several values of the initial magnetization $\mathcal{M}$ under the dark-state condition, with $\chi_2 = -0.01$ and $\delta = 100|\chi_2|$. The stable formation of spinor molecules is possible only for $\mathcal{M} \geqslant 0$.

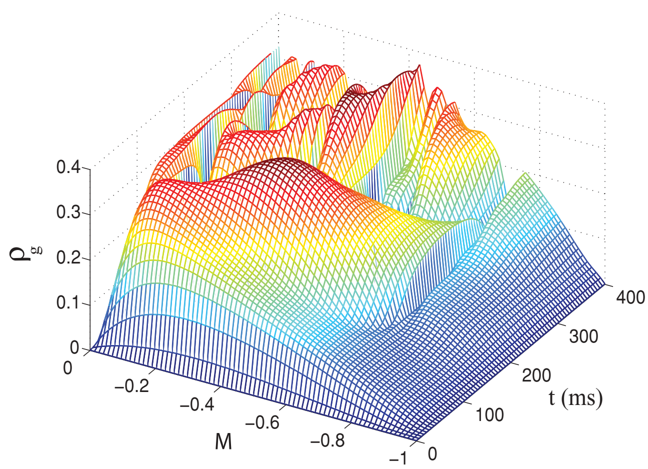

FIG. 5. (Color online) Large-amplitude oscillations of the spinor molecule population for negative values of the magnetization $\mathcal{M} < 0$. All other parameters are as in Fig. 4.

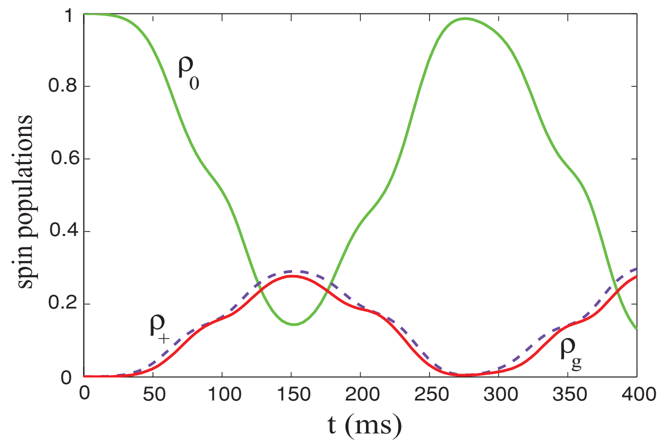

FIG. 6. (Color online) Coherent atom-molecule oscillations as a function of time for ^{87}Rb atoms. The dashed line is the population of the spin-up atoms. The initial atomic state is $f = [0,1,0]$, $\Omega = 0.75|\chi_2|$, and the other parameters are as in Fig. 2.

contrast, this population exhibits large oscillations—see also Fig. 5, which shows more details of the oscillations of ρ_g for negative magnetizations—and does not appear to reach a steady state. This is due to the simple fact that for $\mathcal{M} < 0$, the populations in a spin-down atomic state are not at zero; thus, they are in a "bright" state that does not remain uncoupled from the other atomic states during association.

III. NONRESONANT REGIME

The dynamics of atom-molecule pair formation in the case of negative magnetization indicate that the presence or absence of an atomic dark state plays a key role in that process. In this section, we further investigate the nonresonant situation, where no dark state exists. Specifically, we consider two examples: The first is an "adiabatic" case characterized by an approximate dark-state condition. In this case, the system dynamics can be understood in terms of an effective nonrigid pendulum model that permits us to discuss an antiferromagnetic instability of the atom-molecule pendulum. The second, briefly discussed example is a situation where the dark-state condition is strongly violated.

A. Adiabatic case

Figure 6 shows an example of atom-molecule-pair oscillations for a nonresonant situation and starting from spin-zero ^{87}Rb atoms. (Note that pair formation implies that $\rho_+ \simeq \rho_g$.) As would be intuitively expected, the numerical integration of Eqs. (5) confirms that the creation of atom-molecule pairs is only possible for PA field strengths that allow for the simultaneous occurrence of spin-exchange collisions and atom-molecule conversion. For the initial atomic state $f = [0,1,0]$, we find that the Rabi frequencies of the PA fields should be such that

$$\Omega = -\chi_2\sqrt{\rho_0} \leqslant |\chi_2|$$

or, equivalently,

$$\Omega_1\Omega_2 \leqslant |N\delta c_2|,$$

which gives $\Omega_1 \leqslant 0.3\pi$ MHz and $\Omega_2 \leqslant 0.6\pi$ MHz for the case $\Omega_2/\Omega_1 = 2$ considered here.

We remark that for an atomic condensate initially prepared in the spin-zero state, and assuming that the dark-state condition (8) is approximately satisfied, the first derivatives of the slowly varying amplitudes for spin-down atoms can be neglected, $i\dot{\hat{a}}_- \approx 0$ [24,25]. It is then possible to describe the system by the approximate effective three-state Hamiltonian

$$\begin{aligned}\hat{\mathcal{H}}_{\text{eff}} &= \chi_3\left(\hat{a}_0^{\dagger 3}\hat{a}_+\hat{g} + \hat{a}_0^3\hat{a}_+^\dagger\hat{g}^\dagger\right)\\ &\quad + \frac{1}{\Gamma}\left(\Omega^2\hat{\rho}_0\hat{\rho}_g + \chi_2^2\hat{\rho}_0^2\hat{\rho}_+\right) + \chi_2\hat{\rho}_0\hat{\rho}_+, \qquad (10)\end{aligned}$$

where $\chi_3 = \Omega\chi_2/\Gamma$. The first term in this Hamiltonian describes the creation of atom-molecule pairs from three spin-zero atoms through a laser-induced effective three-body recombination [26].

For short enough times, one could neglect the depletion of the spin-zero population and treat $\hat{a}_0$ as a c number, $\hat{a}_0 \to N^{1/2}$. By linearizing the Hamiltonian (10), the second line then reduces to a self-interacting contribution, with $\Gamma/\rho_0 \simeq \omega - \chi_2$, and the Heisenberg equations of motion for the remaining operators $\hat{a}_+$ and $\hat{g}$ have the solutions

$$\begin{aligned}\hat{a}_+(t) &= \hat{a}_+(0)\cosh\chi_3' t - i\hat{g}^\dagger(0)\sinh\chi_3' t,\\ \hat{g}(t) &= \hat{g}(0)\cosh\chi_3' t - i\hat{a}_+^\dagger(0)\sinh\chi_3' t,\end{aligned} \qquad (11)$$

with $\chi_3' = N^{3/2}\chi_3$. These solutions are well known to be indicative of the quantum entanglement of the created atom-molecule pairs. As such, this system is formally a matter-wave analog of optical parametric down-conversion in quantum optics [1,24].

B. Antiferromagnetic instability

Within the mean-field approach, the spatial part of the atomic and molecular wave functions can be written as $\sqrt{N}e^{-i\mu t/\hbar}\zeta$, where $\zeta = \sqrt{\rho_i}e^{i\theta_i}$ or $\sqrt{\rho_g}e^{i\theta_g}$ and θ_i represents the phase of the ith Zeeman state [3]. Within this description, the dynamics of the system can be expressed in terms of the coupled equations

$$\dot{\rho}_0 = 3\chi_3\rho_0^{3/2}\sqrt{(1-\rho_0)^2-\mathcal{M}^2}\sin\theta,$$
$$\dot{\theta} = -\Theta + \chi_2(1+\mathcal{M}-2\rho_0) + \frac{1}{\Gamma}\bigg[\chi_2^2\rho_0(3+3\mathcal{M}-4\rho_0) + \Omega^2\left(\frac{3}{2}-\frac{3m}{2}-\frac{5\rho_0}{2}\right) + \Omega^2 + (\Delta+\delta-\delta')\Gamma\bigg] + \frac{\Omega\chi_2}{2\Gamma}\frac{\sqrt{\rho_0}[(1-\rho_0)(9-13\rho_0)-9\mathcal{M}^2]}{\sqrt{(1-\rho_0)^2-\mathcal{M}^2}}\cos\theta, \quad (12)$$

where

$$\theta = 3\theta_0 - (\theta_+ + \theta_g) \quad (13)$$

and

$$\Theta = E_g + E_+ - 3E_0. \quad (14)$$

These nonlinear equations support the two phase-independent fixed-point solutions $\rho_0 = 0$ and $\rho_0 = 1-|\mathcal{M}|$, as well as phase-dependent solutions for $\theta = 0$ or π.

Equations (12) describe a nonrigid pendulum with energy functional

$$\mathcal{E} = \lambda_1\cos\theta + \lambda_2, \quad (15)$$

where

$$\lambda_1 = 3\chi_3\rho_0^{3/2}\sqrt{(1-\rho_0)^2-\mathcal{M}^2},$$
$$\lambda_2 = \frac{\rho_0}{\Gamma}\left[\chi_2^2\rho_0\left(\frac{3}{2}+\frac{3}{2}\mathcal{M}-\frac{4}{3}\rho_0\right) + \frac{\Omega^2}{2}\left(3-3\mathcal{M}-\frac{5}{2}\rho_0\right)\right] - \rho_0\left(\Theta+\frac{\Omega^2}{\Gamma}+\Delta+\delta-\delta'\right) + \chi_2\rho_0(1+\mathcal{M}-\rho_0). \quad (16)$$

This approach allows one to simply study the stability of the magnetic domain structure of the system. Specifically, we follow the approach of Ref. [27] and consider instabilities associated with a change in the sign of $d\mathcal{E}/d\mathcal{M}$. For example, $dE/d\mathcal{M} > 0$ for $\mathcal{M} > 0$ and $dE/d\mathcal{M} < 0$ for $\mathcal{M} < 0$ imply that the magnetization always oscillates around zero and no domain forms. Following this approach, we find that, in contrast to the situation for purely atomic gases [27,28], an instability of the domain structure can occur for both ferromagnetic and antiferromagnetic atoms. One readily finds from Eqs. (15) and (16) that

$$\frac{d\mathcal{E}}{d\mathcal{M}} = \frac{3\chi_3}{2}\mathcal{M}\left[1-\frac{\rho_0^{3/2}\cos\theta}{\sqrt{(1-\rho_0)^2-\mathcal{M}^2}}\right] + \chi_2\rho_0 + \frac{3\rho_o}{2\Gamma}(\chi_2^2\rho_0-\Omega^2). \quad (17)$$

Figure 7 shows the resulting surfaces of $d\mathcal{E}/d\mathcal{M} = 0$ for the ferromagnetic and antiferromagnetic cases. The plus or minus sign denotes $d\mathcal{E}/d\mathcal{M} > 0$ or $d\mathcal{E}/d\mathcal{M} < 0$. Here the condensate size is already assumed to be much larger than the healing length $\mathcal{L}_s = 2\pi/\sqrt{2M|c_2'|n}$ at least in one direction, so that instability-induced domains can appear [27].

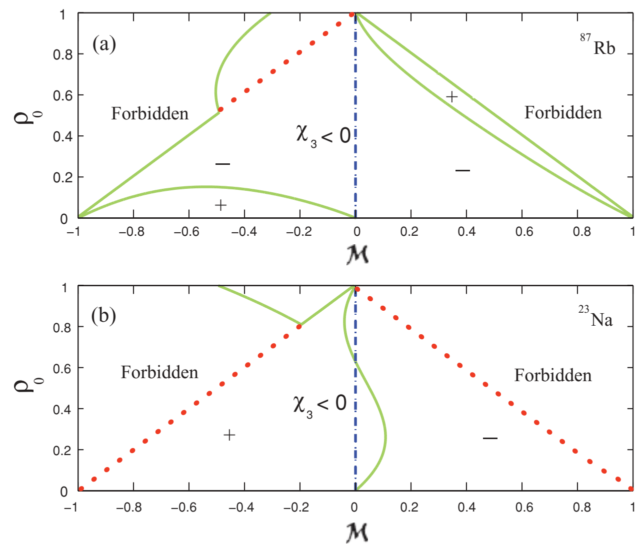

FIG. 7. (Color online) Surfaces of $d\mathcal{E}/d\mathcal{M} = 0$ (green solid lines in online figure) for (a) ferromagnetic ^{87}Rb atoms ($\theta = 0$, $\chi_2 = -0.01$) and (b) antiferromagnetic ^{23}Na atoms ($\theta = \pi$, $\chi_2 = 0.01$). The (red dotted) forbidden lines are determined by the condition of conserved total atomic number or $\rho_0 + |\mathcal{M}| \leqslant 1$ (see Ref. [27]).

As already mentioned, for $d\mathcal{E}/d\mathcal{M} < 0$ an increase in $\mathcal{M}$ leads to lower energy, while for $d\mathcal{E}/d\mathcal{M} > 0$ it leads to a higher energy. Hence, the $(+,-)$ boundary delimits the domain of dynamic instability (see, e.g., Ref. [27] for more details). We observe that in contrast to the case of a pure sample of ^{87}Rb atoms—which is characterized by a wide instability region [27]—in the case at hand, this region can be significantly reduced by an appropriate tuning of the lasers. We also note that in the case of antiferromagnetic atoms such as ^{23}Na, where no dynamical instability exists for a pure atomic sample, with our hybrid system an instability can now develop for a wide range of parameters [see Fig. 7(b)].

One point to emphasize is that antiferromagnetic instability can be experimentally observed without any laser fields—that is, for $\Omega = 0$—although these fields are of course required for the formation of molecules. We also remark that the spin mixing of spin-one molecules is slow enough in comparison with the effective three-body recombination process that it can be safely ignored here. However, thermalization and spontaneous decay of the ground-state molecules are expected to be major challenges for the observation of coherent oscillations of atom-molecule pairs [5].

C. Violation of the dark-state condition

As a final, special case, we now consider the situation where $|\Omega/\chi_2| > 1$, in which case the dark-state condition (8) is completely violated. Figure 8 shows that for increasing values of Ω/χ_2, the amplitude of the oscillations in molecular population first increases and then decreases until $|\Omega/\chi_2| = 1$. Beyond that critical value, the molecular oscillations become strongly damped, and eventually population transfer to the molecular ground state essentially disappears, as illustrated in the figure for $|\Omega/\chi_2| = 1.5$. As illustrated in Fig. 8(b), the

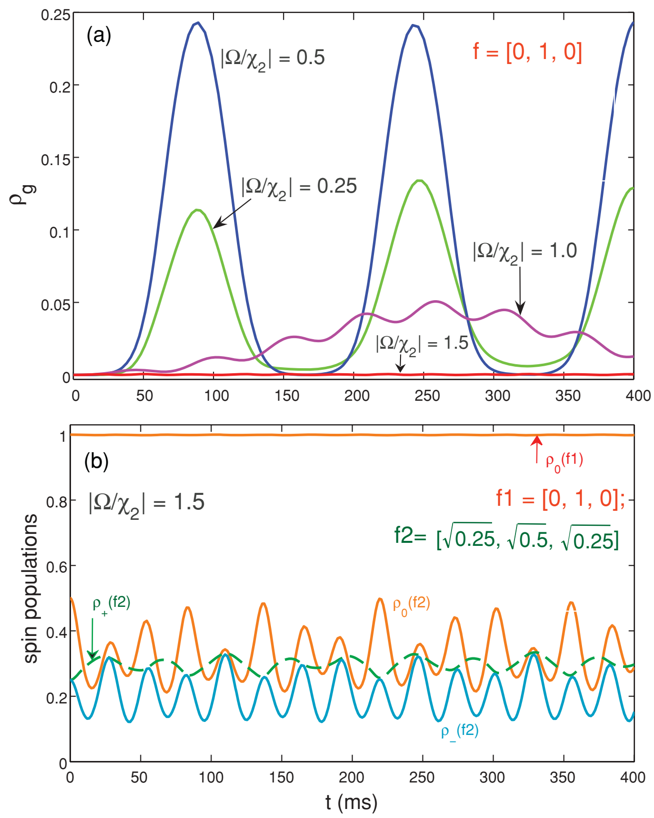

FIG. 8. (Color online) (a) Molecular oscillations for several values of $|\Omega/\chi_2|$, which label the curves, and the initial atomic state $|0,1,0\rangle$. (b) Atomic spin populations for the initial atomic states $|f_1\rangle = |0,1,0\rangle$ and $|f_2\rangle = |\sqrt{0.25},\sqrt{0.5},\sqrt{0.25}\rangle$ and for $|\Omega/\chi_2| = 1.5$. The other parameters are as in Fig. 2.

population oscillations of spin-zero atoms are also strongly suppressed in that regime of strong PA.

Finally, Fig. 8(b) also illustrates how different choices of the initial atomic state result in different dynamics of the spinor atom-molecule system. In particular, an atomic sample initially in the spin-zero state remains completely unperturbed by the strong PA fields (far from the dark-sate resonance condition). Note that the scalarlike atom-molecule conversion illustrated in Fig. 2 corresponds to fields that strongly violate the condition (8), with $|\Omega/\chi_2| = 1.44 \times 10^4 \gg 1$. In that case, the only parameters of practical relevance are the initial atomic state and the strengths of the PA fields.

IV. SUMMARY AND CONCLUSION

In conclusion, we have studied a number of aspects of coherent photo association in a spinor Bose condensate, with emphasis on the creation of atom-molecule pairs from the initial spin-zero atoms. This process, which involves *two* two-body interactions, can be conveniently described by an effective three-body spin-dependent recombination mechanism—the term “three-body recombination” being used here to differentiate our proposal from the recent two-color PA experiment (which involved the scalarlike association of spinor atoms) [16]. We have shown, in particular, that the spin-down atoms can be kept in a dark state for appropriate conditions in both the initial states of the atoms and the PA fields, leading to the formation of atom-molecule pairs. For comparison, we also considered the regimes with PA fields strong enough to violate the dark-state condition.

Although it shares with the previous results similar uses of PA fields and spin-dependent collisions, the present work is nonetheless different from those previous results for laser-catalyzed atomic spin oscillations [17], which did not involve the formation of molecules. In addition, the simulations of experimentally observed scalarlike features in associating spinor atoms, the study of the roles of magnetization and of the initial atomic state, and the antiferromagnetic instability of a hybrid atom-molecule system are also differentiate our results from the previous ones.

In view of the rapid experimental advances in all-optical associations of laser-cooled atoms [19], it can be expected that the coherent PA of quantum spin gases—and in particular, atom-molecule pair formation in a spinor sample—should become experimentally observable in the near future [16]. Laser-controlled spinor reactions can provide a new testing ground to address a number of questions in many-body physics, cold chemistry, and quantum information science. Future work may focus on the creation of heteronuclear spinor molecules from a two-species atomic spin gas [29] and the spinor reactions in an optical lattice [30], with and without long-range dipole-dipole interactions [13]. We also plan to study the cavity-assisted amplification of spinor molecules [31], the bistability of a spinor atom-molecule “pendulum” [32], and spinor trimer formation [20,33].

ACKNOWLEDGMENTS

This work was supported by the U.S. Office of Naval Research, the U.S. National Science Foundation, the U.S. Army Research Office, and the National Science Foundation of China under Grants No. 10874041 and No. 10974045.

[1] P. Meystre, *Atom Optics* (Springer, Berlin, 2001).
[2] J. Stenger, S. Inouye, D. M. Stamper-Kurn, H.-J. Miesner, A. P. Chikkatur, and W. Ketterle, Nature (London) **396**, 345 (1998).
[3] M.-S. Chang, Q. Qin, W. Zhang, L. You, and M. S. Chapman, Nature Phys. **1**, 111 (2005).
[4] M.-S. Chang, C. D. Hamley, M. D. Barrett, J. A. Sauer, K. M. Fortier, W. Zhang, L. You, and M. S. Chapman, Phys. Rev. Lett. **92**, 140403 (2004).
[5] H. Schmaljohann, M. Erhard, J. Kronjäger, M. Kott-ke, S. van Staa, L. Cacciapuoti, J. J. Arlt, K. Bongs, and K. Sengstock, Phys. Rev. Lett. **92**, 040402 (2004); J. Kronjäger, C. Becker, P. Navez, K. Bongs, and K. Sengstock, *ibid.* **97**, 110404 (2006).
[6] A. Griesmaier, J. Werner, S. Hensler, J. Stuhler, and T. Pfau, Phys. Rev. Lett. **94**, 160401 (2005).
[7] T. Ohmi and K. Machida, J. Phys. Soc. Jpn. **67**, 1822 (1998).

[8] T.-L. Ho, Phys. Rev. Lett. **81**, 742 (1998).
[9] C. K. Law, H. Pu, and N. P. Bigelow, Phys. Rev. Lett. **81**, 5257 (1998).
[10] H. Pu, C. K. Law, S. Raghavan, J. H. Eberly, and N. P. Bigelow, Phys. Rev. A **60**, 1463 (1999); W. X. Zhang, D. L. Zhou, M.-S. Chang, M. S. Chapman, and L. You, *ibid.* **72**, 013602 (2005).
[11] B. Sun, W. X. Zhang, S. Yi, M. S. Chapman, and L. You, Phys. Rev. Lett. **97**, 123201 (2006).
[12] A. E. Leanhardt, A. Görlitz, A. P. Chikkatur, D. Kielpinski, Y. Shin, D. E. Pritchard, and W. Ketterle, Phys. Rev. Lett. **89**, 190403 (2002); M. Vengalattore, S. R. Leslie, J. Guzman, and D. M. Stamper-Kurn, *ibid.* **100**, 170403 (2008).
[13] Y. Kawaguchi, H. Saito, and M. Ueda, Phys. Rev. Lett. **96**, 080405 (2006).
[14] R. Dumke, M. Johanning, E. Gomez, J. D. Weinstein, K. M. Jones, and P. D. Lett, New J. Phys. **8**, 64 (2006).
[15] C. D. Hamley, E. M. Bookjans, G. Behin-Aein, P. Ahmadi, and M. S. Chapman, Phys. Rev. A **79**, 023401 (2009).
[16] J. Kobayashi, Y. Izumi, K. Enomoto, M. Kumakura, and Y. Takahashi, Appl. Phys. B **95**, 37 (2009).
[17] H. Jing, Y. Jiang, W. Zhang, and P. Meystre, Phys. Rev. A **81**, R031603 (2010).
[18] J. Cheng, Phys. Rev. A **80**, 023608 (2009); J. Cheng, H. Jing, and Y. J. Yan, *ibid.* **77**, 061604 (2008).
[19] K. Aikawa, D. Akamatsu, M. Hayashi, K. Oasa, J. Kobayashi, P. Naidon, T. Kishimoto, M. Ueda, and S. Inouye, Phys. Rev. Lett. **105**, 203001 (2010).
[20] R. V. Krems, W. C. Stwalley, and B. Friedrich (eds.), *Cold Molecules: Theory, Experiment, Applications* (CRC, Boca Raton, Florida, 2009); L. D. Carr, D. DeMille, R. V. Krems, and J. Ye, New J. Phys. **11**, 055049 (2009).
[21] J. Calsamiglia, M. Mackie, and K. A. Suominen, Phys. Rev. Lett. **87**, 160403 (2001).
[22] K. Winkler, G. Thalhammer, M. Theis, H. Ritsch, R. Grimm, and J. H. Denschlag, Phys. Rev. Lett. **95**, 063202 (2005).
[23] H. Y. Ling, H. Pu, and B. Seaman, Phys. Rev. Lett. **93**, 250403 (2004); J. Cheng, S. S. Han, and Y. J. Yan, Phys. Rev. A **73**, 035601 (2006).
[24] H. Pu and P. Meystre, Phys. Rev. Lett. **85**, 3987 (2000); L. M. Duan, A. Sorensen, J. I. Cirac, and P. Zoller, *ibid.* **85**, 3991 (2000).
[25] Y. X. Liu, J. Q. You, L. F. Wei, C. P. Sun, and F. Nori, Phys. Rev. Lett. **95**, 087001 (2005).
[26] B. Borca, J. W. Dunn, V. Kokoouline, and C. H. Greene, Phys. Rev. Lett. **91**, 070404 (2003); C. P. Search, W. P. Zhang, and P. Meystre, *ibid.* **92**, 140401 (2004).
[27] W. X. Zhang, D. L. Zhou, M.-S. Chang, M. S. Chapman, and L. You, Phys. Rev. Lett. **95**, 180403 (2005).
[28] L. E. Sadler, J. M. Higbie, S. R. Leslie, M. Vengalattore, and D. M. Stamper-Kurn, Nature (London) **443**, 321 (2006).
[29] M. Luo, Z. B. Li, and C. G. Bao, Phys. Rev. A **75**, 043609 (2007).
[30] A. J. Daley, J. M. Taylor, S. Diehl, M. Baranov, and P. Zoller, Phys. Rev. Lett. **102**, 040402 (2009).
[31] C. P. Search and P. Meystre, Phys. Rev. Lett. **93**, 140405 (2004); C. P. Search, J. M. Campuzano, and M. Zivkovic, Phys. Rev. A **80**, 043619 (2009).
[32] Y. Wu and R. Côte, Phys. Rev. A **65**, 053603 (2002); H. Jiang, Y. Jiang, and P. Meystre, *ibid.* **80**, 063618 (2009).
[33] S. Knoop, F. Ferlaino, M. Mark, M. Berninger, H. Schöbel, H.-C. Nägerl, and R. Grimm, Nature Phys. **5**, 227 (2009); F. Ferlaino, S. Knoop, M. Berninger, W. Harm, J. P. D'Incao, H.-C. Nägerl, and R. Grimm, Phys. Rev. Lett. **102**, 140401 (2009); H. Jing, J. Cheng, and P. Meystre, Phys. Rev. A **77**, 043614 (2008).